Helvetica Physica Acta,
Vol. 56 (1983) 463-477

0018-0238/83/010463-15$1.50+0.20/0

HIGH RESOLUTION ELECTRON MICROSCOPY

David J. Smith

High Resolution Electron Microscope, University of Cambridge,
Free School Lane, Cambridge, CB2 3RQ, U.K.

1. Introduction

Recent advances in instrumentation for the electron microscope have resulted in the direct observation of specimen details on the atomic scale, with the increasing availability of high-performance commercial machines leading to a veritable explosion of applications in such diverse fields as solid state chemistry, mineralogy and materials science. In this short review we begin by outlining some of the basic principles of high resolution electron microscopy (HREM), in particular noting some of the restrictions necessarily imposed upon both specimen and microscopist before useful information can be extracted from high-resolution electron micrographs. We then briefly summarise applications of the technique, highlighting some areas where the novel information provided by HREM is causing substantial revision of previous ideas about macroscopic properties. Finally, we discuss likely future developments which should broaden the appeal of the technique to any scientist interested in the structure of materials at the atomic level. Length considerations obviously restrict the details which can be provided here: the interested reader is referred to several recent reviews [1-4], collections of conference papers [5-7] and research monographs [8,9] for further references and other relevant information.

2. Requirements for high resolution

The potential resolution available in the electron microscope arising from sub-Ångstrom electron wavelengths is not realisable in practice because of unavoidable aberrations in the imaging, or objective, lens which restrict the maximum angular aperture of the scattered electrons which can be recombined to form the final image. In practice, resolutions in the 1-3Å range are nowadays routinely available. However, as we will explain, image details on this scale are not easily related to particular features of the specimen under observation. Some appreciation of theoretical background, as

well as instrumentation and operating conditions, is essential for reliable image interpretation. Moreover, lengthy image simulation may often still be required as further confirmation before the nature of inhomogeneities or crystal defects are fully, and unambiguously, characterised.

2.1. Electron-optics and definitions of image resolution. The effect of the objective lens on the image formation process is most conveniently described in terms of its so-called contrast transfer function (CTF), since this is specimen-independent [e.g. 10,11]. For fully coherent, axial illumination, the CTF can be simply represented by the expression

$$\gamma(k) = \exp\{-k^2(k^2/2 - D)\} \quad (1)$$

where k and D are, respectively, the spatial frequency and objective lens defocus in reduced units. i.e. the objective lens can be regarded as acting as a spatial frequency filter with phase changes introduced by spherical aberration (angle-dependent) and defocus. At the optimum defocus, given by $D=(1.5)^{\frac{1}{2}}$, and for a phase object, this expression describes a sine function with a broad band of constant phase which then becomes increasingly oscillatory at higher spatial frequencies (i.e. scattering angles), as shown in Fig.1(a). Thus, electrons scattered to higher angles suffer reversals in phase which can lead to artefacts appearing in the final micrograph. Moreover, in practice, instrumental factors also produce attenuation of this ideal term at higher spatial frequencies which can be represented by further envelope functions [12-14]:

(a) spatial coherence (finite angle of incidence)

$$B(k) = \exp\{-\pi^2 s^2 k^2 (k^2-D)^2\} \quad (2)$$

where s is a generalised co-ordinate representing illumination divergence ;

(b) temporal coherence (finite spread of focus)

$$C(k) = \exp\{-\pi^2 d_o^2 k^2/2\} \quad (3)$$

where d_o represents the effective half-width of the focal spread distribution, and includes contributions from the finite energy spread of the beam, as well as high voltage and lens current instabilities. The typical combined effects of these envelope functions on the CTF are shown in Fig.1b. Finally, it should be noted that, because of CTF variations, the high-resolution electron micrograph varies rapidly with defocus; many image artefacts, including contrast reversals, will appear in a focal series of images.

The form of the CTF with partially coherent illumination, as shown in Fig.1, provides straightforward definitions for image resolution. The

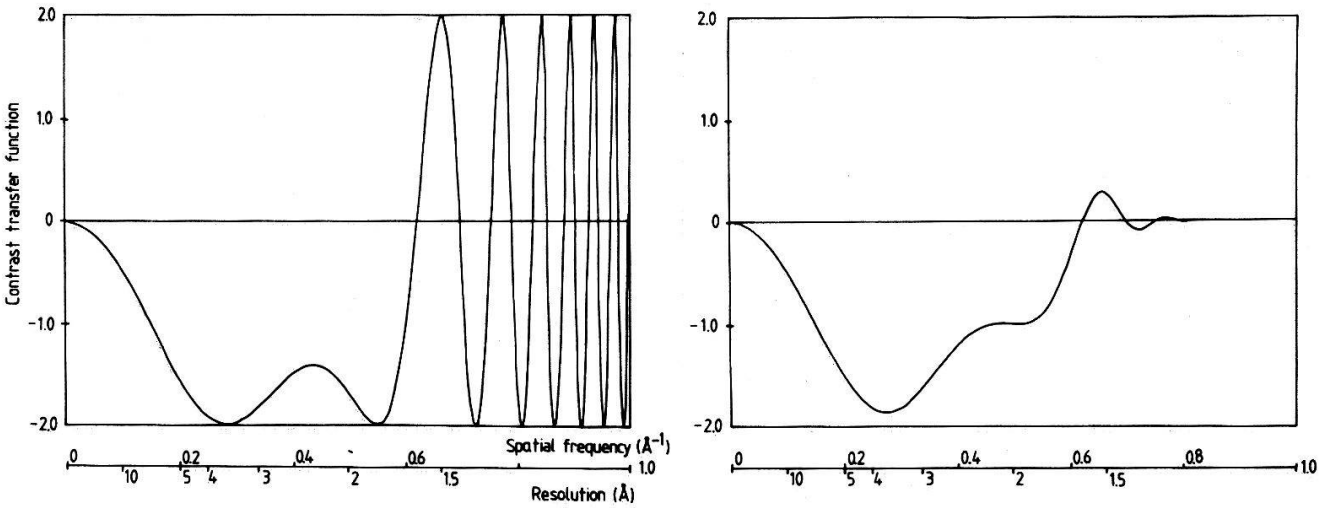

Fig.1. Contrast transfer functions for a high resolution electron microscope at 500kV; C_s=2.0mm, axial illumination. (a) coherent illumination; (b) effect of damping functions: incident semi-angle 0.4mrad, focal spread 100Å.

"interpretable resolution" corresponds to the widest band of spatial frequencies without phase reversals occurring at the optimum defocus position. In "real" units, this resolution is given approximately by the expression

$$\delta \sim 0.7 C_s^{1/4} \lambda^{3/4} \qquad (4)$$

where C_s is the spherical aberration coefficient of the objective lens and λ is the electron wavelength. Typical values of δ are shown in Table I. Intuitive image interpretation to this resolution in terms of the projected atomic distribution in the sample are sometimes possible. The "instrumental resolution" is defined in terms of the attenuation produced by the envelope functions with exp(-2) (i.e. 15%) normally taken as the cut-off limit for which a posteriori image processing might usefully be applied to deconvolute the effect of the CTF and to retrieve specimen information [15]. It is common with 100 and 200kV microscopes for the instrumental resolution to be considerably better than the interpretable resolution although the reverse appears to be true of high voltage instruments [16]. However, the image artefacts which are present in the former cases make image simulation essential before any detailed image interpretation is attempted.

TABLE I

Interpretable resolution for various λ and C_s-values

kV	λ(Å)	C_s(mm)	δ(Å)
100	0.0370	0.7	3.0
200	0.0251	1.2	2.5
600	0.0126	2.0	1.8
1000	0.0087	3.0	1.5

Finally, it is appropriate to distinguish the above resolution limits from the common, though often misleading, "lattice fringe resolution". For both interpretable and instrumental resolutions, there exist firm theoretical bases (see 2.4 below) for relating details of an image obtained under certain well-defined operating conditions with specimen features of the same resolution. Lattice fringes, such as those shown in Fig.2, simply reflect the existence of two, or sometimes more, diffracted beams passing through the back focal plane of the objective lens which have been re-combined to form an interference fringe pattern. Such diffracted beams arise from comparatively large specimen areas (perhaps 20Å or more across) and thus do not convey information about individual atomic arrangements. Alternatively, however, it must be noted that the finest spacings visible in these interference fringes represent a sensitive test of instrumental stability, both mechanical and magnetic, as well as depending on adequate illumination coherence. Spacings as fine as 0.63Å have been reported from a 100kV microscope [17] despite a corresponding value for δ of about 3Å.

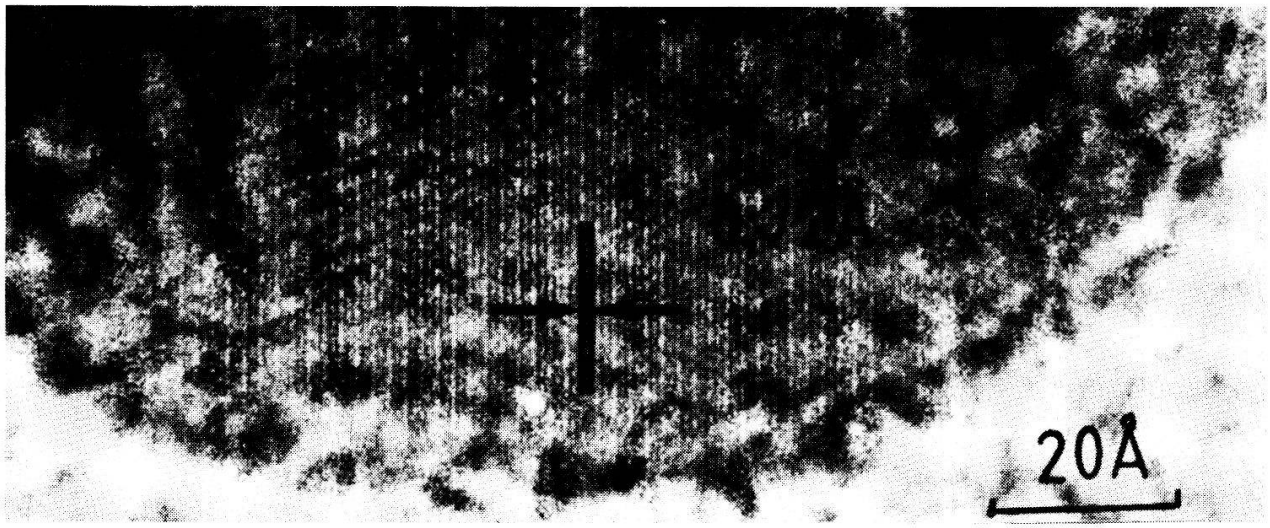

Fig.2. Small particle of silver imaged at 575kV showing 0.72Å lattice fringes arising from interference of (220) and ($2\bar{2}0$) beams [18].

2.2. Instrumentation Whilst imaging theory is now well-established, it has only been comparatively recently that basic instrumentation for the electron microscope has been adequate for producing, and recording, direct information about atomic arrangements. For example, the specimen stage must allow the material under observation to be precisely positioned (to several tens of Ångstroms at most) and accurately oriented (to $\sim 10^{-3}$ rad or better) and yet, at the same time, to be effectively free of any lateral drift during photographic exposures (typically $\sim$0.1Å/sec or less). Furthermore, the microscope itself

must be isolated from sources of mechanical vibration, as well as stray alternating fields, and high voltage and lens current instabilities must be around 1 part per million. Commercial instruments currently available have most of these adventitious factors under control although our experience suggests [19] that it is still prudent to have facilities on-hand for monitoring the most critical parameters, namely high voltage stability, vibration levels and stray magnetic fields in case there should be any deterioration in performance.

From (4) above, it is apparent that there are only two options available for improving the value of δ, the interpretable resolution. Current 100 and 200kV HREMs typically have minimum C_s values of 0.7 and 1.2mm respectively and any further reductions appear likely to be marginal given the minimal space currently available for the specimen (tilt angles restricted to ±12°) and the highly-saturated condition of the objective lens pole-pieces. The only prospect at these voltages is that there might be some breakthrough in the recent efforts at aberration correction using complicated multipole lenses [20,21]. There is a gradual increase in C_s-values, because of saturation,as the electron accelerating voltage is raised. However, as demonstrated in Table I, this is more than offset by the reduction in electron wavelength with the net result that δ improves considerably. Moreover, since pole-piece dimensions are increased, the problems of specimen manipulation are somewhat eased with tilt angles of ±30°, for example, becoming easily obtainable. This marked improvement in potential resolution has provided the motivation for the recent construction of several high voltage microscopes dedicated to high resolution [19, 22-26]. However, the problems of mechanical and electrical stabilities associated with these necessarily much larger instruments have made this goal difficult to realise on a routine basis [27].

2.3. Specimen preparation and modes of operation. In order for atomic-level structural information to become obtainable in the HREM, specimen thicknesses of 100Å or less are typically required. In such thin regions it is regrettably likely that some of the defect structures observed, for example dislocations, will be atypical of bulk structure. Moreover, irrespective of the method of preparation, whether by electrolytic, chemical or ion-beam thinning or by the standard grinding techniques used for many brittle inorganic materials, it is quite common for the local crystal orientation to vary considerably, expecially in the vicinity of defects. In such

cases, selected area electron diffraction patterns, typically originating from regions 0.5 microns or more across, are not useful as more than rough guides for tilting purposes; it is then helpful to have available some computed image simulations showing the expected appearance of perfect crystal regions.

Whilst imaging with an axial incident beam in the conventional transmission electron microscope (CTEM) can give straightforward image interpretation, it should also be appreciated that there are other operating modes which can provide image detail at the atomic level under certain specific conditions. For example, tilted illumination offers the possibility of an improvement in "resolution" well beyond the corresponding value of δ, although only in one direction, and this mode can then be used in 100kV microscopes for the imaging of one-dimensional lattice fringes from metallic specimens (see, for example, [28]). However, the corresponding imaging theory becomes much more complicated [13] and it is very difficult to obtain reliable quantitative information about local specimen features, such as dislocations [29], on the same scale.

Finally, mention should be made of the scanning transmission electron microscope (STEM). Unlike the CTEM which uses a stationary electron beam illuminating a large specimen area (perhaps 0.5-1 micron in diameter), the high-resolution STEM involves a small probe (perhaps 5Å in diameter) moving in raster-like fashion across a sample, with synchronous collection of transmitted electrons and signal display on a monitor. By reciprocity, the imaging theory applicable to the CTEM can also be shown to be valid for the STEM [30]. However, the high-resolution capabilities of the STEM has so far only been really effective in imaging isolated atoms or clusters [31,32] rather than extended specimens although, as described later in Section 4, the multi-signal output, coupled with the small probe size, can supply other valuable specimen information.

2.4. Image interpretation and simulation As already noted above, imaging theory (see, for example, [8,9 and 13]) is in a comparatively advanced state when compared with the instrumentation side of HREM. Indeed, computer programs based on the multi-slice formulation of n-beam dynamical theory [33] were in existence a decade ago [34] which could reliably simulate, albeit slowly, the images only very recently starting to be obtained experimentally. Moreover, the theory can also be used rigorously to define the experimental

conditions, especially specimen thickness, necessary for obtaining micrographs which are directly interpretable in terms of specimen features, i.e. when there is a linear relationship between image intensity and the projected potential of the specimen.

In the simplest approach, the specimen is assumed to be thin enough for it to be considered as a weak phase object. It then has the transmission function

$$t(\underline{r}) = \exp\{-i\sigma\phi(r)\} \approx 1-i\sigma\phi(\underline{r}) \qquad (5)$$

where $\phi(\underline{r})$ represents the projection of the scattering potential in the beam direction and σ the so-called interaction constant. This term is then modulated in phase and amplitude by the CTF term described by (1), before propagation through the microscope (which can be considered as equivalent to successive Fourier transformations) first to arrive at the diffracted amplitudes, and finally to give the image amplitude. This weak phase object approximation, discussed in detail elsewhere [for example, 8,13,35 and 36] is strictly only valid at 100kV for atoms of medium atomic number for thicknesses less than 10 to 30Å and perhaps only monolayers of very heavy atoms. This approximation also remains valid for increased thicknesses, at equivalent resolution, as the accelerating voltage is raised [4]. Furthermore, despite Fresnel diffraction effects which spread the electron beam side sideways as it traverses a sample, as well as multiple scattering by the sample, it has been found [4] that some qualitative agreement between the experimental micrograph and image simulation often remains up to substantially thicker specimens. Unfortunately, however, in this thickness regime where the image is only related non-linearly to the object no universal generalisations about image interpretability can safely be made: image simulations should again be regarded as essential. Finally, a thickness is reached where, except for a few isolated cases, image simulations no longer resemble the experimental micrographs. This is primarily because, as well as multiple elastic scattering, considerable inelastic scattering also occurs and there is currently no satisfactory way of including its effect. The interested reader is referred to a recent review [37] where the prospects for "deciphering" micrographs obtained from thicker regions have been considered.

As well as helping to define the experimental conditions valid for intuitive image interpretation, particularly the allowable ranges of defocus and specimen thickness, image simulations are indispensable to defect

characterisation as well as structure determination. For example, image matching of perfect crystal regions neighbouring a defect of interest can provide an accurate estimate of the prevailing imaging conditions, including the extent of the damping functions, the objective lens defocus, the C_s-value and the specimen thickness [38]. In turn, knowledge of these parameters greatly facilitates the otherwise very tedious task of obtaining an image match which (hopefully) discriminates between alternative defect models. The similarity in appearance of experimental and simulated images has also been used as the criterion for a structure determination of the complex inorganic oxide "$GeNb_9O_{25}$" [39].

3. Applications

The presence and nature of any structural irregularities in a material generally have a great influence on its macroscopic behaviour. High resolution electron microscopy, unlike other bulk diffraction techniques, is able to provide localised specimen information on the atomic scale, making it a powerful technique for characterising materials. Thus, in many crystalline substances, where linear or planar faults are projected to be parallel with the incident beam direction, the detailed atomic configurations around the lattice defects can be imaged directly. In "amorphous" materials, the presence of any ordered regions might be detected. The ready availability of such information, albeit within the constraints of resolution and thickness mentioned above, accounts for the increasingly widespread use of HREM in laboratories throughout the world.

Although the original demonstrations of lattice resolution in the electron microscope came with the work of Menter [40], it was not until considerably later, after advances in both instrumentation and theoretical understanding, that a direct correspondence was established between fringe images and projected crystal lattice geometry [41]. Iijima [42] later obtained the first images showing the individual atomic columns in the complex inorganic oxide $Ti_2Nb_{10}O_{29}$. Since the structure of this material was well-known from X-ray diffraction, image simulations were able to confirm the validity of the image interpretation, and thereby provide confidence for the subsequent observation of related materials, particularly those having lattice defects. In the latest high-voltage instruments [19, 22-26], interpretable resolutions are now better than 2Å, making it possible to observe individual atomic columns directly even in the low index zones of close-

packed metals.

A wide variety of materials and defects are thus becoming amenable to characterisation in the high-resolution electron microscope. These include [see also 5-7, 19 and 24]:

- ceramics, such as SiC and Si-Al-O-N phases;
- semiconductors, such as Si, GaAs and CdTe;
- catalysts, and small particles generally;
- oxide and metallic glasses;
- alloy systems, particularly superlattice phases and anti-phase domains;
- nonstoichiometric oxides, such as TiO_{2-x} and WO_{3-x};
- silicate and carbonate minerals;
- molecular crystals, such as aromatic hydrocarbons and phthalocyanines.

The various morphological features of interest include the atomic arrangements at dislocations as well as at planar faults such as twin boundaries, interfaces and shear planes; the nature of point defects (interstitial or vacancy type); the surface and internal structure of catalysts and small metal particles; and the presence of impurity phases possibly segregated at any linear or planar defects. Finally, of course, observation of these various features at the atomic level provides unique insights into numerous physical and chemical processes. A non-exhaustive list includes:

- the development of nonstoichiometry;
- epitaxy;
- crystal growth;
- phase transformations;
- corrosion and/or oxidation;
- precipitation;
- ion implantation.

It is not our objective here to provide comprehensive details of all these HREM applications. Instead, we will briefly describe a few representative examples to illustrate both the power of the technique and its likely impact.

(a) ion-implantation. The technique of implantation with high-energy ions is widely used as a means of favourably altering various physical properties such as surface hardness and electrical conductivity. In the electronics industry, it is also used, prior to subsequent annealing treatment, to amorphise device materials such as the silicon in silicon-on-sapphire (SOS) wafers which has a high defect density in the as-prepared state. Whilst

immediate interest focusses on the morphology of the final annealed wafers [43], particularly of the Si-crystallinity, preliminary images of the implanted wafer, in cross-sectional view, are potentially of great significance. Fig.3 shows, for example, the transition region between the crystalline surface seed and the bulk amorphised layer. Small crystallites are visible, surrounded by amorphous regions, which clearly retain the bulk silicon lattice spacing and orientation. Such images indicate that HREM will allow the effects of implantation on the implanted material to be studied directly at the lattice resolution level.

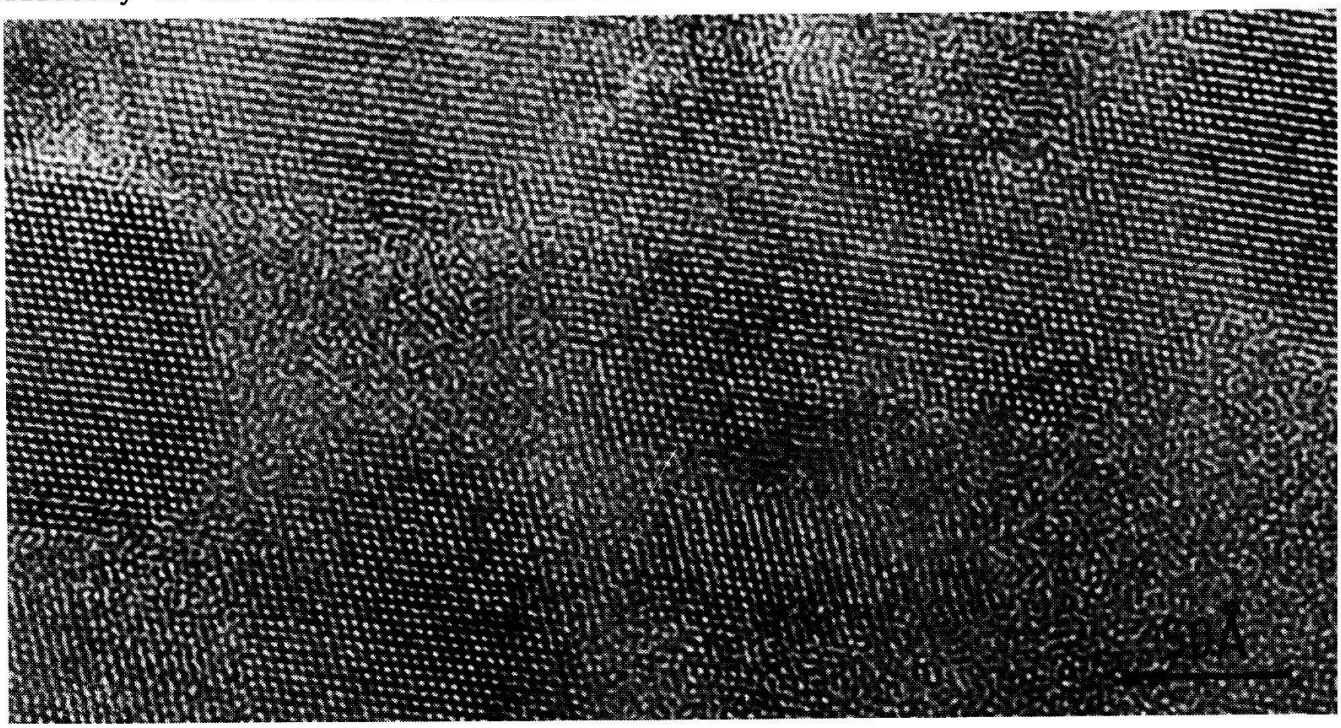

Fig.3. Ion-implanted silicon showing transition region between amorphised bulk crystal and the crystalline surface layer [43].

(b) nonstoichiometric rutile. Recent HREM observations of slightly-reduced rutile, TiO_{2-x} ($0 \leq x \leq 0.0035$), have established a number of novel structural features not revealed by earlier low-resolution studies, including the existence of {100} platelet defects, longitudinal and lateral disorder in the fine structure of crystallographic shear planes (CSP), and the absence of CSP in quenched specimens [44]. These results have forced the development of new structural models for cation interstitial and anion vacancy defects [45], and it is anticipated that these will account for a number of point-defect phenomena associated with rutile as well as being applicable to other non-stoichiometric oxide systems. Similar extensive disorder along CSP has also been observed in samples of chromia-doped rutile, $Ti(Cr)O_{1.92}$, despite the

the apparently well-ordered superstructures suggested by electron diffraction patterns [46]. However, as shown in Fig.4, excellent agreement between experimental micrographs and computer simulations can still be achieved.

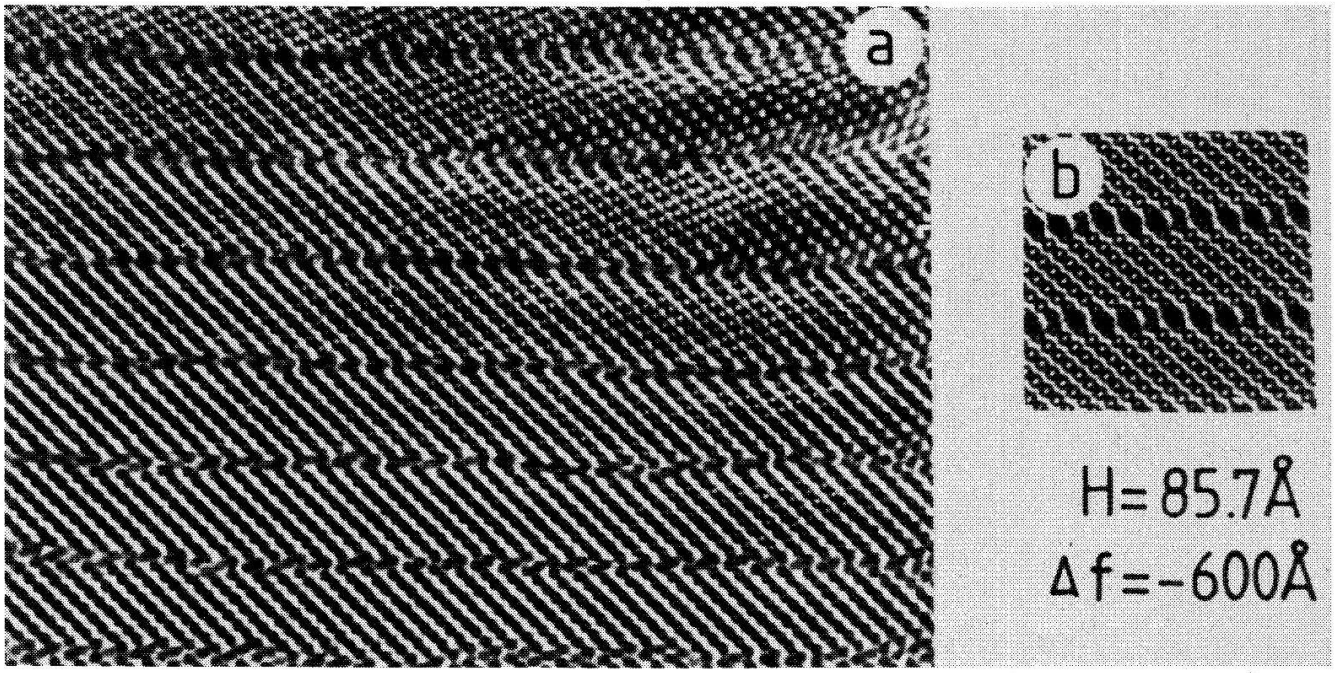

Fig.4. Comparison between (a) experimental micrograph (500kV, $C_s \sim 2.7$mm), and (b) computer simulation, of ordered 374 crystallographic shear structure. Focus and thickness shown [46].

(c) surface imaging of small metal particles. Knowledge of the internal and surface structure of small metal particles is crucial to understanding their role in heterogeneous catalysis. Recent HREM observations have established the existence of dislocations within the particles [47] and provided images of particle surfaces clearly displaying the facetting of surface steps and some evidence for surface reconstruction [48]. Moreover, image simulations, taking proper account of edge-termination effects, have confirmed the validity of image interpretation in terms of separate atomic columns. For example, the small particle of gold, shown in Fig.5, has a partially-reconstructed (2x1) surface superstructure which closely matches the appearance of the (inset) image simulation corresponding to the so-called "missing-row model" [49], with the black spots in the periodic arrays representing individual rows of gold atoms viewed end-on. This demonstrated ability to study particle morphologies at the atomic level, as well as changes therein, should prove of enormous value to catalysis and surface science studies generally although, as noted below, there is a need for better control of the microscope environment around the specimen.

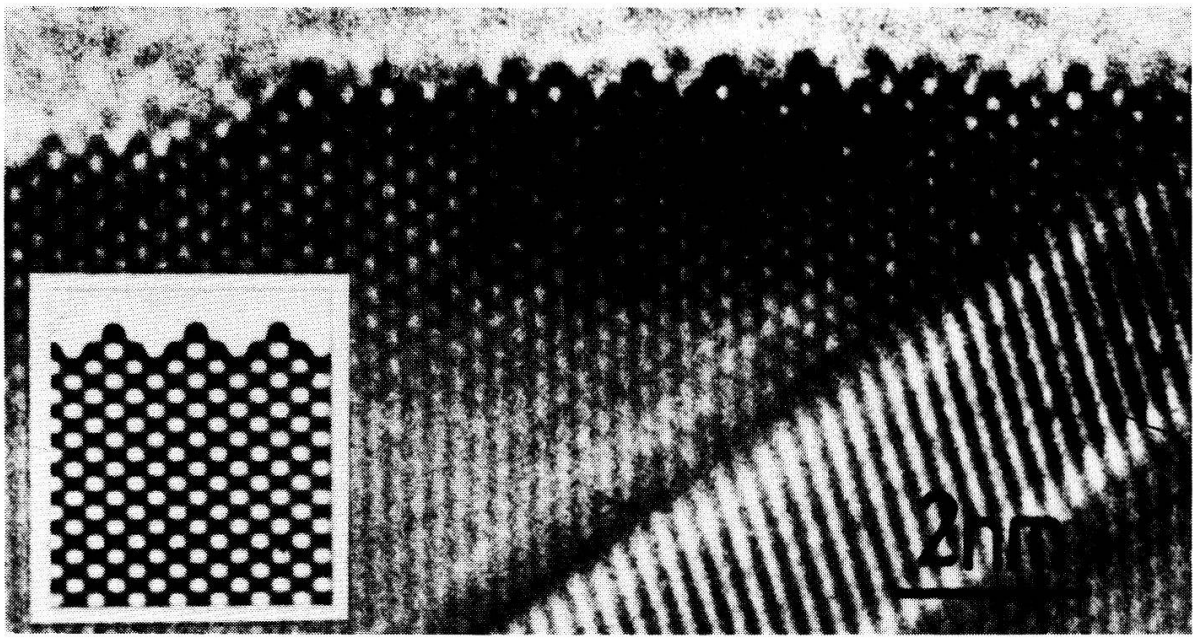

Fig.5. Small particle of gold showing directly, at the atomic level, a partially-reconstructed (2x1) surface superstructure [48]. Inset shows simulation corresponding to the "missing-row" model [49].

4. Future developments

The information "immediately" available from HREM observations can be usefully augmented and extended in several different ways. Attachment of an image pickup and display system [50-52], for example, not only provides a valuable aid for image viewing and focussing, particularly under low light level viewing conditions, but also offers the possibility for observing, recording and analysis of dynamic events [53,54], as well as on-line digital computer processing with the aid of a so-called framestore system [51,52]. Indeed, it has recently been demonstrated [55] that focussing, stigmating and incident beam alignment can be carried out routinely using a minicomputer, with a precision generally better than that attained by highly-experienced operators. Increasing use of computers for microscope operation, as well as for on-line signal processing, can be anticipated in future thereby enabling the microscopist to concentrate more on the materials under examination.

The high-resolution electron micrograph can not directly provide information concerning the component elements of a specimen, although this knowledge is often crucial to structure determinations, identification of precipitates, etc. However, the electron beam excites several different, but characteristic, signals as it traverses a sample and these can be used

instead as a means if identification. The primary method for this microanalysis involves energy-dispersive X-ray spectroscopy (EDS), usually with a solid-state detector placed to the side of the specimen. Previously, it has been accepted that provision of the detector would result in loss of image resolution, but this is gradually being overcome by careful design, as well as by the use of higher voltage instruments (eg. 200kV) where the space around the specimen is less cramped because of increased pole-piece dimensions. A second microanalytical technique, namely electron energy loss spectroscopy (EELS), involves the use of a magnetic sector spectrometer to measure the energy spectrum of the electron beam emerging from the specimen. The form of this EELS spectrum again readily identifies the atomic species present, even those light elements such as carbon and oxygen where EDS is relatively insensitive. Each technique has its own particular merits in different applications, discussed in detail elsewhere [56], but clearly the addition of both facilities to the HREM would provide additional chemical information complementary to that obtainable by HREM about local atomic arrangements. Finally, we note that use of the stationary probe of the STEM would enable microanalysis from much smaller regions. For this reason, there will be mounting pressure for hybrid instruments which combine the highest possible CTEM resolution with the very small probe sizes available in the STEM mode.

Facilities for controlling and modifying the physical and chemical environment of samples within the electron microscope have been in existence for some time, but, because of space considerations, these have always been associated with lower performance instruments. Better design and improved pumping systems are leading to cleaner microscope columns so that contamination is no longer a problem even when small specimen areas are irradiated. Moreover, as microscope vacuums approach the UHV-level, comprehensive surface studies involving in situ heating/cooling and evaporations should be possible in most high-resolution instruments [57], rather than only those which have been custom-built for that purpose [25]. Goniometer (tilting) stages are also becoming available which will permit these treatments without serious loss of resolution. Direct observation of the atomic re-arrangements associated with these various in situ experiments should significantly enhance our knowledge and understanding of many chemical reactions.

5. Conclusions.

The practical realisation of atomic-level resolutions in the electron microscope has been a considerable technological achievement. Moreover, the principles of microscope operation and image interpretation are now well-understood. The challenge now rests with the electron microscopist to take full advantage of this powerful technique for investigating the basic microstructure of materials.

Acknowledgement

Financial support from the Science and Engineering Research Council is gratefully acknowledged.

References

[1] D.J. SMITH, V.E. COSSLETT & W.M. STOBBS, Interdisc.Sci.Revs.6,155 (1981)
[2] W. NEUMANN, M. PASEMANN & J. HEYDENREICH, in Crystals, Growth, Properties and Applications, Vol.7. 1 (Springer-Verlag, Berlin, 1982)
[3] S. PENNYCOOK, Contemp. Phys. 23, 371 (1982)
[4] J.M. COWLEY, Ultramicroscopy 8, 1 (1982)
[5] Direct Imaging of Atoms in Crystals and Molecules (Proc. 47th Nobel Symposium 1979) Ed. by L. KIHLBORG (Royal Swedish Academy of Sciences and the Nobel Symposium: Stockholm) (also appeared as Chemica Scripta, Vol. 14, 1978/79)
[6] Ultramicroscopy, Vol. 8. No.1 (1982)
[7] J. Microscopy, Vol. 129, No.3 and Vol. 130, Nos. 2 and 3 (1983)
[8] J.M. COWLEY, Diffraction Physics (North Holland, Amsterdam, 1975)
[9] J.C.H. SPENCE, Experimental High-Resolution Electron Microscopy (Clarendon, Oxford, 1981)
[10] F. THON, Z. Natursforsch, A21, 476 (1966)
[11] K.-H. HANSZEN, Adv. Opt. Electron Micr. 4, 1 (1971)
[12] J. FRANK, Optik 38, 519 (1973)
[13] W.O. SAXTON, Computer Techniques for Image Processing in Electron Microscopy (Academic, New York, 1978)
[14] D.J. SMITH, in Electron Microscopy 1980, Vol. 4, pp. 126-133
[15] C.J. HUMPHREYS & J.C.H. SPENCE, Optik 58, 125 (1981)
[16] D.J. SMITH, R.A. CAMPS & L.A. FREEMAN, Inst. Phys. Conf. Ser.61, 381
[17] A. TONOMURA, T. MATSUDA, J. ENDO, H. TODOKORO & T. KOMODA, J. Electron Micr. 28, 1 (1979)
[18] D.J. SMITH, R.A. CAMPS, L.A. FREEMAN, R. HILL, W.C. NIXON & K.C.A. SMITH, J. Microscopy 130, 127
[19] D.J. SMITH, R.A. CAMPS, V.E. COSSLETT, L.A. FREEMAN, W.O. SAXTON, W.C. NIXON, H. AHMED, C.J.D. CATTO, J.R.A. CLEAVER, K.C.A. SMITH & A.E. TIMBS, Ultramicroscopy 9, 203 (1982)
[20] H. KOOPS, in Electron Microscopy 1978, Vol. 3, pp. 185-196
[21] A.V. CREWE, Optik 60, 271 (1982)
[22] K. KOBAYASHI, E. SUITO, N. UYEDA, M. WATANABE, T. YANAKA, T. ETOH, H. WATANABE, & M. MORIGUCHI, in Electron Microscopy 1974, Vol.1, pp. 30-31
[23] S. HORIUCHI, Y. MATSUI, Y. BANDO, T. KATSUTA & I. MATSUI, J. Electron Mic. 27, 389 (1978)

[24] M. HIRABAYASHI, K. HIRAGA & D. SHINDO, Ultramicroscopy 9, 197 (1982)
[25] G. HONJO, K. YAGI, K. TAKAYANAGI, S. NAKAGURA, S. KATAGIRI, M. KUBOZOE & I. MATSUI, in Electron Microscopy 1980, Vol. 4. pp.22-25
[26] R. GRONSKY, in Proc. 38th Ann. Meet. EMSA, Ed. by G.W. BAILEY (Claitors, Baton Rouge, 1980) pp. 2-5
[27] D.J. SMITH, in Proc. 38th Ann. Meet. EMSA, Ed. by G.W. BAILEY (Claitors, Baton Rouge, 1980) pp. 822-825
[28] P.G. SELF, H.K.D.M. BHADESHIA & W.M. STOBBS, Ultramicroscopy 6, 29 (1981)
[29] D.J. COCKAYNE, J.R. PARSONS & C.W. HOELKE, Phil. Mag. 24, 139 (1971)
[30] J.M. COWLEY, Appl. Phys. Letts. 15, 58 (1969)
[31] A.V. CREWE, J.S. WALL & J.P. LANGMORE, Science 168, 1338 (1970)
[32] M. ISAACSON, D. KOPF, M. UTLAUT, N.W. PARKER & A.V. CREWE, Proc. Nat. Acad. Sci. USA, 74. 1802 (1971)
[33] J.M. COWLEY & A.F. MOODIE, Acta Cryst. 10, 609 (1957)
[34] P. GOODMAN & A.F. MOODIE, Acta Cryst. A30, 280 (1974)
[35] J.M. COWLEY, in Principles and Techniques of Electron Microscopy, Vol.6, Ed. by M.A. HAYAT (Van Nostrand Reinhold, New York, 1976) pp. 40-84
[36] D.L. MISELL, Image Analysis, Enhancement and Interpretation; in Practical Methods in Electron Microscopy, Vol.7, Ed. by A.M. GLAUERT (North-Holland, Amsterdam, 1978)
[37] W.O. SAXTON, J. Micr. Spectrosc. Electron. 5, 661 (1980)
[38] A.R. WILSON, A.E.C. SPARGO & D.J. SMITH, Optik 61, 63 (1982)
[39] A.J. SKARNULIS, S. IIJIMA & J.M. COWLEY, Acta Cryst. A32, 799 (1976)
[40] J.W. MENTER. Proc. Roy. Soc. London. Ser.A,236, 119 (1956)
[41] J.G. ALLPRESS, J.V. SANDERS & D.W. WADSLEY, Acta Cryst. B25, 1156 (1969)
[42] S. IIJIMA, J. Appl. Phys. 42, 5891 (1971)
[43] D.J. SMITH, L.A. FREEMAN, R. MCMAHON, H. AHMED, M.G. PITT & T.B. PETERS in Microscopy of Semiconducting Materials III, Ed. by A.G. Cullis (Institute of Physics, Bristol and London, 1983) in press
[44] L.A. BURSILL, M.G. BLANCHIN & D.J. SMITH. Proc. Roy. Soc. Lond. Ser. A, 384, 135 (1982)
[45] L.A. BURSILL & M.G. BLANCHIN, J. de Physique (Lettres) 44, L165 (1983)
[46] G.J. WOOD, L.A. BURSILL & D.J. SMITH, J. Microscopy, 129, 263 (1983)
[47] D.J. SMITH & L.D. MARKS, Phil. Mag. A44, 735 (1981)
[48] L.D. MARKS & D.J. SMITH. Nature, in press (1983)
[49] H.P. BONZEL & S. FERRER, Surface Science 118, L263 (1982)
[50] K.-H. HERRMANN, D. KRAHL & H.-P. RUST, Ultramicroscopy, 3, 227 (1978)
[51] E.D. BOYES, B.J. MUGGRIDGE, M.J. GORINGE, J.L. HUTCHISON & G. CATLOW, Inst. Phys. Conf. Ser. 61, 119 (1982)
[52] C.J.D. CATTO, K.C.A. SMITH, W.C. NIXON, S.J. ERASMUS & D.J. SMITH, Inst. Phys. Conf. Ser. 61, 123 (1982)
[53] R. SINCLAIR, F.A. PONCE, T. YAMASHITA, D.J. SMITH, R.A. CAMPS, L.A. FREEMAN, S.J. ERASMUS, W.C. NIXON, K.C.A. SMITH & C.J.D. CATTO, Nature 298, 127 (1982)
[54] F.P. OTTENSMEYER, D.P. BAZETT JONES, H.-P. RUST, K. WEISS, F. ZEMLIN & A. ENGEL, Ultramicroscopy 3, 191 (1978)
[55] W.O. SAXTON, D.J. SMITH & S.J. ERASMUS, J. Microscopy 130, 187 (1983)
[56] L.M. BROWN, J. Phys. F: Metal Phys.11, 1 (1981)
[57] K. TAKAYANAGI, in Electron Microscopy 1982, Vol.1, pp. 43-50